Thoracic CT-PET Registration Using a 3D Breathing Model

Antonio Moreno[1], Sylvie Chambon[1], Anand P. Santhanam[2,3], Roberta Brocardo[1], Patrick Kupelian[3], Jannick P. Rolland[2], Elsa Angelini[1], and Isabelle Bloch[1]

[1] Ecole Nationale Supérieure des Télécommunications (GET - Télécom Paris), CNRS UMR 5141 LTCI - Signal and Image Processing Department, Paris, France
[2] Optical Diagnostics and Application Laboratory, University of Central Florida
[3] Department of Radiation Oncology, MD Anderson Cancer Center Orlando, USA

Abstract. In the context of thoracic CT-PET volume registration, we present a novel method to incorporate a breathing model in a non-linear registration procedure, guaranteeing physiologically plausible deformations. The approach also accounts for the rigid motions of lung tumor during breathing. We performed a set of five registration experiments on a healthy and four pathological data set. Initial results demonstrate the interest of this method to significantly improve the multi-modality volume registration for diagnosis and radiotherapy applications.

1 Introduction

Registration of multimodal medical images is a widely addressed topic in many different domains, in particular for oncology and radiotherapy applications. We consider Computed Tomography (CT) and Positron Emission Tomography (PET) in thoracic regions, which provide complementary information about the anatomy and the metabolism of the human body (Fig. 1). Their registration has a significant impact on improving medical decisions for diagnosis and therapy [1–3]. Linear registration is not sufficient to cope with local deformations produced by respiratory motions. Even with combined PET/CT scanners (which avoid differences in patient orientation and provide linearly registered images), non-linear registration remains necessary to compensate for cardiac and respiratory motions [4].

Most of the existing non-linear registration methods are based on image information and do not take into account any knowledge of the physiology of the human body. Landmark-based registration techniques do take physiology into account by forcing homologous points to match. In this direction, several papers present breathing models built for medical visualization but few papers exploit such models in a registration process (Section 2).

In this paper, we propose an approach in which we integrate a physiologically driven breathing model into a 3D non-linear registration procedure in order to guarantee physiologically plausible deformations (Sections 3 and 4). The registration problem is defined between two CT volumes and one PET volume

(Fig. 1). Even if PET images are often blurred and represent an average volume throughout the respiratory cycle, we assume that, using a breathing model, we can compute a CT volume that can be closer to the PET volume than the original CT volumes.

Fig. 1. CT images (a,b) corresponding to two different instants of the breathing cycle and PET image (c) of the same patient (coronal views).

2 Breathing Models and Thoracic Imaging Registration

Currently, respiration-gated radiotherapies are being developed to improve the efficiency of radiations of lung (or abdominal) tumors [5]. Three techniques have been proposed so far: (i) *active techniques* controling the patient's breathing (airflow is blocked); (ii) *passive or empirical techniques* using external measurements in order to adapt radiation protocols to the tumor's motion [6–8]; (iii) *model-based techniques* employing a breathing model to evaluate lungs deformations during the breathing cycle [9].

We focus on thoracic volume registration and made a "patient-specific" registration through the use of a breathing model. Different bio-mathematical representations of the human respiratory mechanics have been developed [10]. *Mathematical tools* can be employed for medical visualization. The most popular techniques are based on Non-Uniform Rational B-Spline (NURBS). NURBS surface is a bidirectional parametric representation of an object. In [11], NURBS surfaces have been used to correct for respiratory artifacts of SPECT images. This model is called NCAT (NURBS-based cardiac-torso). A multi-resolution registration approach for 4D Magnetic Resonance Imaging (MRI) is proposed in [12]. In [13], a 4D NCAT phantom and an original CT are used to generate 4D CT and to compute an elastic registration. *Physically-based models* describe the important role of airflow inside the lungs and can be based on Active Breathing Coordinator (ABC, it allows clinicians to pause a patients breathing at a precisely indicated tidal volume) [9] or volume preservation relation [14, 15].

In [16], segmented MRI are used in order to simulate PET volumes at different instants of the respiration cycle. These estimated PET volumes are used to evaluate different PET/MRI registration processes. Authors of [17, 12] use pre-register MRI to estimate the breathing model. A CT registration using a breathing model is presented in [9] but a specific equipement is needed. In [13], the NCAT phantom is used, but, from a modeling and simulation point of view, physically-based deformation methods are better adapted for simulating lung

dynamics as they allow precise generation of intermediate 3D lung shapes. They are easy to adapt to patient, without the need for physical external adaptations.

Physics-Based Dynamic 3D Surface Lung Model – An approach was previously discussed in [15] and the two major components involved in the modeling and visualization efforts include: (1) Parameterization of PV (Pressure Volume) data from a human subject which acts as an ABC; (2) Estimation of the deformation operator from 4D CT lung data sets.

In step (1) a parameterized PV curve, obtained from normal human subjects, is used as a driver for simulating the 3D lung shapes at different lung volumes. In step (2), the computation takes as inputs the nodal displacements of the 3D lung models and the estimated amount of force applied on the nodes of the meshes (which are on the surface). Displacements are obtained from 4D CT of a normal human subject. The direction and magnitude of the lung surface point's displacement are computed using the volume linearity constraint, i.e. the fact that the expansion of lung tissues is linearly related to the increase in lung volume. The estimated amount of applied force on each node (that represents the air-flow inside lungs) is estimated based on a PV curve and the lungs's orientation with respect to the gravity, which controls the air flow. Given these inputs, a physics-based deformation approach based on Green's function (GF) formulation is estimated to deform the 3D lung surface models. Specifically the GF is defined in terms of a physiological factor, the regional alveolar expandability (elastic properties), and a structural factor, the inter-nodal distance of the 3D surface lung model. To compute the coefficients of these two factors, an iterative approach is employed and, at each step, the force applied on a node is shared with its neighboring nodes based on a local normalization of the alveolar expandability coupled with inter-nodal distance. The process stops when this sharing of the applied force reaches equilibrium. Validation of lung deformations using 4D CT datasets is described in [18].

3 Combining Breathing Model and Image Registration

We have conceived an original algorithm in order to incorporate breathing model described above in our multimodal image registration procedure. Fig. 2 shows the computational workflow of the complete algorithm. The input consists of one PET volume and two CT volumes of the same patient, corresponding to two different instants of the breathing cycle (end-inspiration and end-expiration, for example, collected with breath-hold maneuver). The preliminary step consists in segmenting the lung surfaces (and, eventually, the tumors) on the PET data and on the two CT data sets, using a robust mathematical-morphology-based approach [19], and extracting meshes corresponding to the segmented objects.

Computation of a Patient-Specific Breathing Model – For each patient, we only have two segmented CT lung datasets, therefore we first estimate the intermediate 3D lung shapes between these two datasets. Then, displacements of lung surface points are computed as follows:

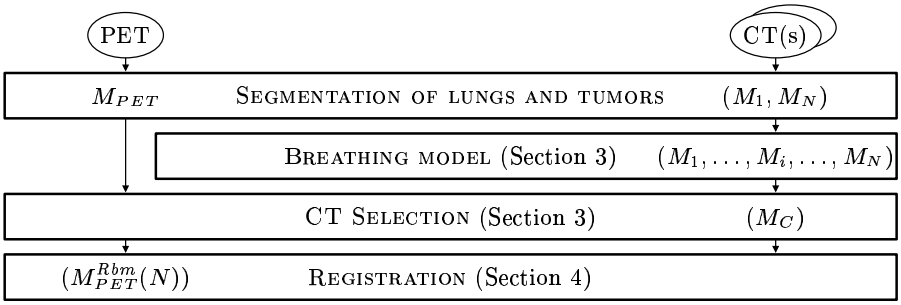

Fig. 2. Registration of CT and PET volumes using a breathing model.

(1) *Directions* are given by the model (computed from a 4D CT normal data set of reference).
(2) *Magnitudes* are "patient-specific" and are computed from the given 3D CT lung datasets.

In other words, for known directions of displacement the magnitude of the displacement is computed from the two 3D CT lung datasets. With known estimations of applied force and "subject-specific" displacements the coefficients of the GF can be estimated (Section 2). Then, the GF operator is used to compute the 3D lung shapes at different intermediate lung volumes.

CT Selection – By applying the continuous breathing model, we obtain different instants ("snapshots") of the breathing cycle, generating simulated CT meshes. By comparing each CT mesh with the PET mesh, we select the "closest" one (i. e. with the most similar anatomy). Let us denote the CT simulated meshes M_1, M_2,..., M_N with M_1 corresponding to the CT in maximum exhalation and M_N to maximum inhalation. By using the breathing model, the transformation $\phi_{i,j}$ between two instants i and j of the breathing cycle can be computed as: $M_j = \phi_{i,j}(M_i)$. We compare these CT meshes with the PET mesh (M_{PET}) based on a measure of similarity C. The mesh that minimizes C (here the root mean square distance) is denoted as M_C: $M_C = \arg\min_i C(M_i, M_{PET})$.

Deformation of the PET – A *direct* registration, denoted f^{Rd}, can be computed between M_{PET} and the original CT mesh M_N (dashed line in Fig. 3): where $M_{PET}^{Rd}(N)$ is the result of registering the PET directly to the CT mesh M_N. The transformation f^{Rd} may be computed by any registration method adapted to the problem (note that this could be done with another instant M_i). In this *direct* approach the deformation itself is not guided by any anatomical knowledge. In addition, if the PET and the original CT are very different, it is likely that this registration procedure will provide physically unrealistic results.

To avoid such potential problems, we propose here an alternative approach: once the appropriate CT (M_C) is selected, we compute the registration, f^r,

between the M_{PET} mesh and the M_C mesh as:

$$M^r_{PET}(C) = f^r(M_{PET}, M_C), \tag{1}$$

where $M^r_{PET}(C)$ denotes the registered mesh. Then, the transformation due to the breathing is used to register the PET to the original CT (continuous line in Fig. 3) incorporating the known transformation between M_C and M_N:

$$\Phi_{C,N} = \phi_{N-1,N} \circ \ldots \circ \phi_{C+1,C+2} \circ \phi_{C,C+1}. \tag{2}$$

We apply $\Phi_{C,N}$ to $M^r_{PET}(C)$ in order to compute the registration with M_N:

$$M^{Rbm}_{PET}(N) = \Phi_{C,N}(M^r_{PET}) = \Phi_{C,N}(f^r(M_{PET}, M_C)), \tag{3}$$

where $M^{Rbm}_{PET}(N)$ denotes the PET registered mesh using the breathing model.

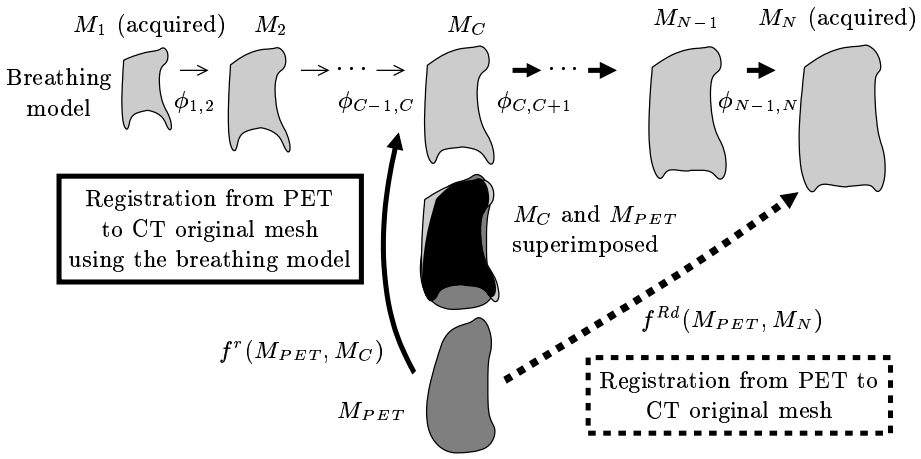

Fig. 3. Registration framework on PET (M_{PET}) and CT mesh (M_N) – The M_C mesh is the closest to the M_{PET} mesh. We can register M_{PET} to the M_N mesh (original CT) following one of the two paths.

4 Registration Method Adapted to Pathologies

The algorithm described in Section 3 can be applied with any type of registration method, i.e. f^{Rd} and f^r may be computed by any registration method adapted to the problem. We show here how the proposed approach can be adapted for registration of multi-modality images in pathological cases.

Registration with Rigidity Constraints – We have previously developed a registration algorithm for the thoracic region in the presence of pathologies taking into account the presence of tumors, while preserving continuous smooth deformations [20]. We assume that the tumor is rigid and that a linear transformation is sufficient to cope with its displacements between CT and PET scanning. This hypothesis is relevant and in accordance with the clinicians' point of view, since tumors are often compact masses of pathological tissue. The registration algorithm relies on segmented structures (lungs and tumors). Landmarks points are defined in both datasets to guide the deformation of the PET volume towards the CT volume. The deformation at each point is computed using an interpolation procedure, the specific type of deformation of each landmark depending on the structure it belongs to, and weighted by a distance function, which guarantees continuity of the transformation.

Registration with Rigidity Constraints and Breathing Model – When the different CT meshes are computed and the closest CT mesh, M_C, is selected, we register the PET and the original CT (in our example M_N) with the following procedure:

(1) Selection of landmark points on the CT mesh M_C (based on Gaussian and mean curvatures and uniformly distributed on the lung surface) [21];
(2) Estimation of corresponding landmark points on the PET mesh M_{PET} (using the Iterative Closest Point (ICP) algorithm [22]);
(3) Tracking of landmark points from M_C to the CT mesh M_N using the breathing model;
(4) Registration of the PET and the original CT using the estimated correspondences with the method summarized in the previous paragraph.

The breathing model used in step (3) guarantees that the corresponding landmarks selected on the original CT are correct (and actually they represent the same anatomical point) and follow the deformations of the lungs during the respiratory cycle.

5 Results and Discussion

We have applied our algorithm on a normal case and on four pathological cases, exhibiting one tumor. In all the cases, we have one PET (of size $144 \times 144 \times 230$ with resolution of $4 \times 4 \times 4$ mm or $168 \times 168 \times 329$ with resolution of $4 \times 4 \times 3$ mm) and two CT volumes (of size $256 \times 256 \times 55$ with resolution of $1.42 \times 1.42 \times 5$ mm to $512 \times 512 \times 138$ with resolution of $0.98 \times 0.98 \times 5$ mm), acquired during breath-hold in maximum inspiration and in intermediate inspiration, from individual scanners. The breathing model was initialized using the lung meshes from the segmented CT. Ten meshes (corresponding to regularly distributed instants) were generated and compared with the PET. The computing time can be of two hours for the whole processing (a few seconds for segmentation, a few minutes for landmark detection and about one hour and half for the registration). Although

this is not a constraint because we do not deal with an on-line process, we can optimize this computing cost.

As illustrated in Fig. 4 and 5 (one normal case and one pathological case), the correspondences between landmark points on the original CT and the PET are more realistic in the results obtained with the breathing model (images (e) and (f)) than without (images (b) and (c)). Using the model, it can be observed that the corresponding points represent the same anatomical points and that the uniqueness constraint is respected, leading to visually better looking PET registered images. In particular, the lower part of the two lungs is better registered using the model (the lung contour in the registered PET is closer to the lung contour in the original CT). In the illustrated pathological case, the tumor is well registered and not deformed. Moreover, the distance between the registered PET lungs and the original CT lungs is loewr than using the direct approach.

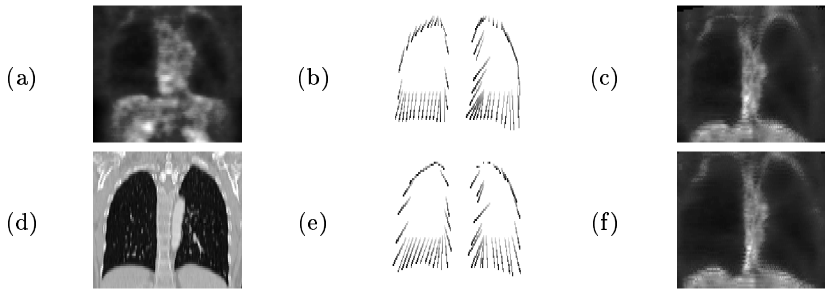

Fig. 4. Original PET (a) and CT (d) images in a normal case. The correspondences between the selected points in the PET image and in the CT image are shown in (b) and (e) (corresponding points are linked). Registered PET is shown in (c) for the direct method and in (f) for the method with the breathing model.

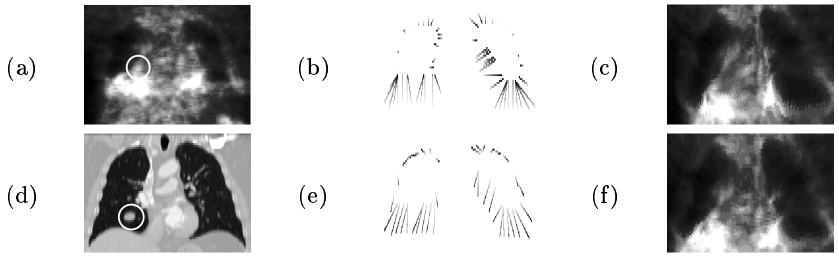

Fig. 5. Original PET (a) and CT (d) images in a pathological case (the tumor is surrounded by a white circle). The correspondences between the selected points in the PET image and in the CT image are shown in (b) and (e) (correspondent points are linked). The registration result is shown in (c) for the direct method and in (f) for the method with the breathing model.

In this paper, we consider the impact of the physiology on lung surface deformation, based on reference data of normal human subjects. Therefore the methodology presented in this paper will further benefit upon the inclusion of patho-physiology specific data once established. The use of normal lung physiology serves to demonstrate improvements in CT and PET registration using a physics-based 3D breathing lung model. Current work includes a quantitative comparison and evaluation on a larger database, in collaboration with clinicians.

References

1. Lavely *et al.*, W.: Phantom validation of coregistration of PET and CT for image-guided radiotherapy. Medical Physics **31**(5) (2004) 1083–1092
2. Rizzo *et al.*, G.: Automatic registration of PET and CT studies for clinical use in thoracic and abdominal conformal radiotherapy. Physics in Medecine and Biology **49**(3) (2005) 267–279
3. Vogel *et al.*, W.: Correction of an image size difference between positron emission tomography (PET) and computed tomography (CT) improves image fusion of dedicated PET and CT. Physics in Medecine and Biology **27**(6) (2006) 515–519
4. Shekhar *et al.*, R.: Automated 3-Dimensional Elastic Registration of Whole-Body PET and CT from Separate or Combined Scanners. The Journal of Nuclear Medicine **46**(9) (2005) 1488–1496
5. Sarrut, D.: Deformable registration for image-guided radiation therapy. Zeitschrift für Medizinische Physik **13** (2006) 285–297
6. McClelland *et al.*, J.: A Continuous 4D Motion Model from Multiple Respiratory Cycles for Use in Lung Radiotherapy. Medical Physics **33**(9) (2006) 3348–3358
7. Nehmeh *et al.*, S.: Four-dimensional (4D) PET/CT imaging of the thorax. Physics in Medecine and Biology **31**(12) (2004) 3179–3186
8. Wolthaus *et al.*, J.: Fusion of respiration-correlated PET and CT scans: correlated lung tumour motion in anatomical and functional scans. Physics in Medecine and Biology **50**(7) (2005) 1569–1583
9. Sarrut *et al.*, D.: Non-rigid registration method to assess reproducibility of breath-holding with ABC in lung cancer. International Journal of Radiation Oncology–Biology–Physis **61**(2) (2005) 594–607
10. Mead, J.: Measurement of Inertia of the Lungs at Increased Ambient Pressure. Journal of Applied Physiology **2**(1) (1956) 208–212
11. Segars *et al.*, W.: Study of the Efficacy of Respiratory Gating in Myocardial SPECT Using the New 4-D NCAT Phantom. IEEE Transactions on Nuclear Science **49**(3) (2002) 675–679
12. Rohlfing *et al.*, T.: Modeling Liver Motion and Deformation During the Respiratory Cycle Using Intensity-Based Free-Form Registration of Gated MR Images. Medical Physics **31**(3) (2004) 427–432
13. Guerrero *et al.*, T.: Elastic image mapping for 4-D dose estimation in thoracic radiotherapy. Radiation Protection Dosimetry **115**(1–4) (2005) 497–502
14. Zordan *et al.*, V.: Breathe Easy: Model and Control of Human Respiration for Computer Animation. Graphical Models **68**(2) (2006) 113–132
15. Santhanam, A.: Modeling, Simulation, and Visualization of 3D Lung Dynamics. PhD thesis, University of Central Florida (2006)

16. Pollari *et al.*, M.: Evaluation of cardiac PET-MRI registration methods using a numerical breathing phantom. In: IEEE International Symposium on Biomedical Imaging. (2004) 1447–1450
17. Sundaram, T., Gee, J.: Towards a Model of Lung Biomechanics: Pulmonary Kinematics Via Registration of Serial Lung Images. Medical Image Analysis **9**(6) (2005) 524–537
18. Santhanam *et al.*, A.: Modeling Simulation and Visualization of Real-Time 3D Lung Dynamics. IEEE Transactions on Information Technology in Biomedicine (2007) In press.
19. Camara *et al.*, O.: Explicit Incorporation of Prior Anatomical Information into a Nonrigid Registration of Thoracic and Abdominal CT and 18-FDG Whole-Body Emision PET Images. IEEE Transactions on Medical Imaging (2007) To appear.
20. Moreno *et al.*, A.: Non-linear Registration Between 3D Images Including Rigid Objects: Application to CT and PET Lung Images With Tumors. In: Workshop on Image Registration in Deformable Environments (DEFORM), Edinburgh, UK (2006) 31–40
21. Moreno *et al.*, A.: CT-PET Landmark-based Lung Registration Using a Dynamic Breathing Model. In: International Conference on Image Analysis and Processing, Modena, Italy (September 2007) To appear.
22. Besl, P., McKay, N.: A Method for Registration of 3-D Shapes. IEEE Transactions on Pattern Analysis and Machine Intelligence **14**(2) (1992) 239–256